

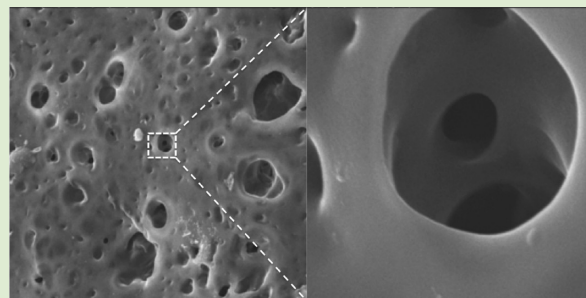
## Stimuli-Responsive Nanolatexes: Porating Films

Dustin England,<sup>†</sup> Nikhil Tambe,<sup>‡</sup> and John Texter\*

Coatings Research Institute, School of Engineering Technology, Eastern Michigan University, Ypsilanti, Michigan 48197, United States

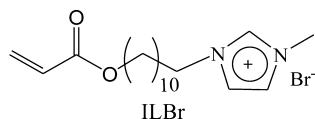
## S Supporting Information

**ABSTRACT:** A new class of very stable and stimuli-responsive nanolatexes based on copolymers of reactive and stimuli responsive ionic liquid surfactants is synthesized by microemulsion polymerization to yield dispersions of 22–30 nm diameter particles. Aqueous coatings of these nanolatexes dry to form robust films that exhibit stimuli-responsiveness to certain ion exchangeable anions. The nature of the reactive ionic liquid surfactant monomers induces an ion exchange capacity in the resulting copolymers and films. Transparent films of such nanolatexes can be transformed into opaque and porous films and membranes as a stimulus-response to anion exchange. These nanolatexes are ionic nanogels that are insensitive to Debye–Hückel screening by an indifferent salt and exhibit very soft interparticle interactions, qualifying them as ideal candidates as waterborne dispersing aids; in addition, these nanogels appear to be experimental examples of osmotic nanospheres emanating from the theoretical development of osmotic brushes.



Porosity in coatings has been found useful in diverse applications including anticorrosion treatments,<sup>1</sup> antislip coatings,<sup>2</sup> perfumed coatings,<sup>3</sup> and antireflective coatings.<sup>4–7</sup> Coating is generally done in order to preserve or protect a substrate from environmental effects. Semipermeable coatings, however, can provide barriers to certain components and fields while allowing certain chemical components to easily pass, and porosity in coatings can provide desired optical effects, changes in interfacial adhesion, and a variety of flow and filtration effects. Porosity in latex coatings involves exceeding the critical pigment concentration,<sup>8</sup> using porous pigments,<sup>9</sup> or otherwise has included incorporation of some sort of poragen.<sup>5,10</sup>

In this study we follow the report of Yan and Texter of nanolatexes derived from the ionic liquid surfactant acrylate, ILBr with MMA (methylmethacrylate) comonomer, and that exhibited colloidal stability in high salt.<sup>11</sup> Nanolatexes in this system were prepared at the 0.07/0.07/0.86 ILBr/MMA/water weight ratio composition. These latexes were about 40 nm in diameter and were found to be very stable. By very stable we mean that they appeared *immune to coagulation* by indifferent salt (or by salt-induced shrinking of the Debye–Hückel screening layer) and were colloidally stable in 0.1 M NaBr, wherein the Debye–Hückel length is only 1 nm.<sup>12,13</sup>



Latexes generally maintain their stability through charge repulsion.<sup>14</sup> When the chemical environment changes, such as with the introduction of an indifferent salt, the particles can lose their stability; increasing solution ionic strength causes the

electrical double layer of the stabilized latex particles to compress. This shrinking reduces the energetic barrier to aggregation and coagulation. The ILBr monomer consists of a hydrophilic, cationic imidazolium headgroup and a hydrophobic tail tipped with acrylate. It was expected that the polymerized nanolatex particles were primarily stabilized by the cationic charge located near the surface. This preservation of stability in the presence of high salt content suggested that these nanolatex particles were sterically stabilized. These more recently prepared nanolatex compositions were further tested in aqueous solutions of stimuli-responsive anions to determine the respective concentrations needed for destabilization. They were also examined as film formers and to see if the resulting films exhibited any of the interesting poration phenomena exhibited by similarly composed gels.<sup>11,15</sup>

Nanolatex suspensions were prepared by microemulsion polymerization<sup>16</sup> of solutions initially formulated at nominally 2, 3, and 4% ILBr by weight (w/w) with MMA as a comonomer at 2/3 the amount of ILBr. The detailed procedure is given in the Supporting Information (SI) and yielded nanolatex particles in the 20–30 nm size range as indicated by dynamic light scattering measurements.<sup>16</sup> TEM of the nanolatexes are shown in the SI. The small size is unusual<sup>17</sup> for thermal polymerization, but is aided in this case by a small amount of cross-linker we believe to be an *N,N*-bis-(acryloylundecyl)imidazolium bromide impurity in the ILBr synthesis (see SI).

Received: December 19, 2011

Accepted: January 17, 2012

Published: January 26, 2012

Aqueous NaBr solutions (3 mL) were prepared with concentrations ranging from 0.1–1.0 M. About 0.7 mg of total nanolatex solids were added to each of these solutions, and turbidity was determined visually both immediately and 1 h after addition of nanolatex. Turbidity measurements were then made at 800 nm using a Jasco UV/vis spectrophotometer. These turbidity measurements<sup>18</sup> are illustrated in Figure 1. The

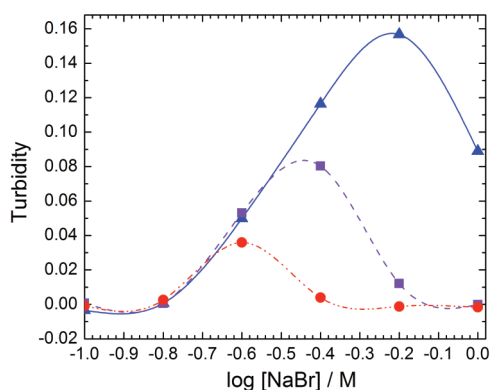


**Figure 1.** Turbidity at 800 nm of dialyzed nanolatexes added to aqueous NaBr after equilibration for 1 h. Nanolatexes formulated at 2% (blue triangle), 3% (purple square), and 4% (red circle) ILBr.

increasing turbidity with NaBr concentration is due to the increasing rate of coagulation induced by bromide interacting with the imidazolium cation and decreasing the effective stabilization. The subsequent falloff in turbidity is due to the aggregation being so substantial that the aggregates sedimented to the bottom of the vial prior to our being able to measure the turbidity. Similar measurements were made for Na<sub>2</sub>S, NaBF<sub>4</sub>, and KPF<sub>6</sub> (see SI).

These visual and UV/vis estimates of the destabilization concentrations are summarized in Table 1. We see that both

**Table 1. Destabilization Concentrations for Nanolatexes in Various Aqueous Salts for “4%” ILBr Nanolatexes**

salt	visual destabilization concentration (M)	UV/vis destabilization concentration (M)
NaBr	0.21 ± 0.06	0.24 ± 0.06
NaBF <sub>4</sub>	7.4 × 10 <sup>-3</sup> ± 3.7 × 10 <sup>-3</sup>	9.4 × 10 <sup>-3</sup> ± 2.7 × 10 <sup>-3</sup>
KPF <sub>6</sub>	3.5 × 10 <sup>-4</sup> ± 1.8 × 10 <sup>-4</sup>	4.0 × 10 <sup>-4</sup> ± 8.7 × 10 <sup>-5</sup>
Na <sub>2</sub> S	1.6	1.8

forms of estimation indicate these anions interact in the following sequence of decreasing strength: PF<sub>6</sub><sup>-</sup> > BF<sub>4</sub><sup>-</sup> > Br<sup>-</sup> > S<sup>2-</sup>. These interactions are founded in equilibrated binding to the imidazolium ring.<sup>19–22</sup> The range of destabilizing concentrations is 0.35 mM to 1.8 M, or about 4 orders of magnitude. The ionic strength of 1 M Na<sub>2</sub>S is 3 M. These nanolatexes are stable in such an ionic strength, so we can conclude steric stabilization dominates the stabilization mechanism. Only 0.35 mM KPF<sub>6</sub> is destabilizing, and this is due to specific interactions between the PF<sub>6</sub><sup>-</sup> anion and the imidazolium ring.

SEM was also used to study the formation of pores in a 4% ILBr undialyzed nanolatex film treated with 0.1 M KPF<sub>6</sub> to induce ion exchange, and thus local pore formation, presumably through spinodal decomposition.<sup>15</sup> The first film analyzed (Figure 2) was cast in a PTFE mold, and the second film (Figure 3) was made by drawing down the nanolatex on a glass microscope slide (see SI for lower magnifications). The

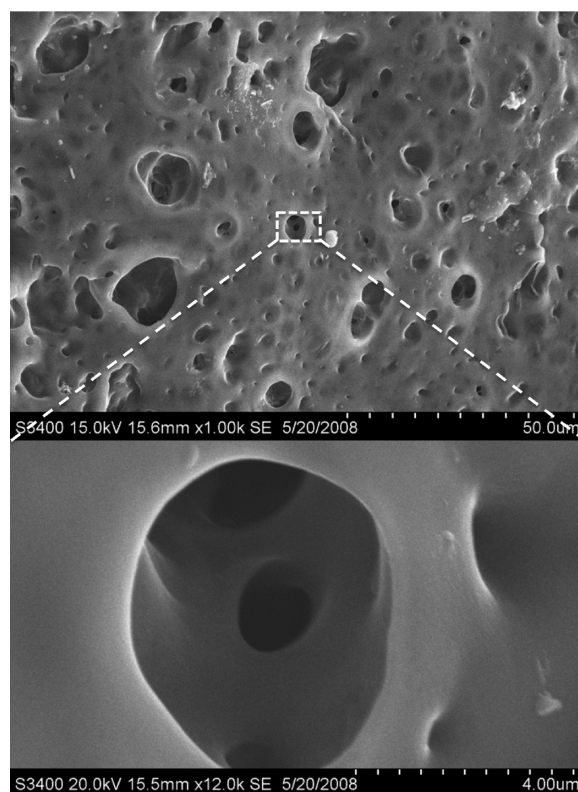


**Figure 2.** SEM images of 4% ILBr (undialyzed) nanolatex film, peeled from a PTFE mold and treated with 0.1 M KPF<sub>6</sub>. The top image shows a region of the freeze fractured cross-sectional surface. The lower image is a magnification of one of the pores shown in the top image.

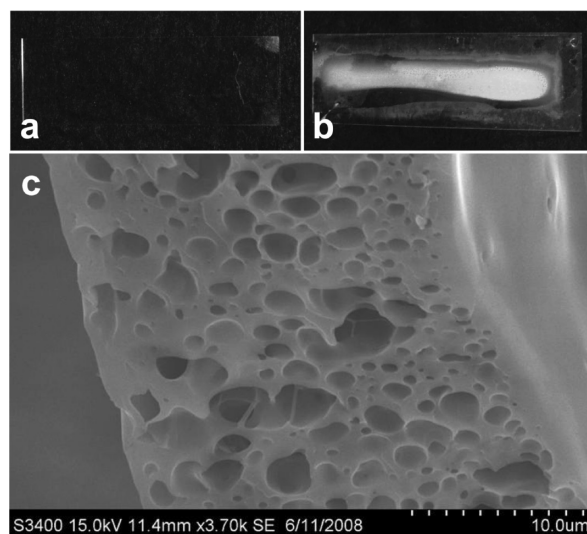


**Figure 3.** SEM of 4% ILBr undialyzed nanolatex coating on a glass slide before (a) and after (b) treatment with 0.1 M KPF<sub>6</sub>; (c) SEM image of film shaving fracture surface.

transparent film peeled from the PTFE mold became opaque after overnight equilibration in aqueous KPF<sub>6</sub>, suggesting the formation of light scattering pores. Once rinsed, the film was dried, submerged in liquid nitrogen, and freeze fractured to produce a cross-sectional surface to analyze by SEM. The film exhibited open-cell pore structures (Figure 2) on both outer surfaces and across the entirety of the cross-sectional fracture

surface, suggesting that the  $\text{KPF}_6$  solution was able to diffuse throughout the thin film.

The film produced by drawing down a 4% ILBr nanolatex on a glass slide was also equilibrated for several days in 0.1 M  $\text{KPF}_6$ , resulting in an opaque film (Figure 3). This film was then immersed in liquid nitrogen while still attached to the slide. Once frozen, shavings of the film were scraped by razor blade and then freeze fractured. Similar to the cast film, open-cell pore networks were observed on the outer surfaces as well as throughout the cross-sectional fracture surface illustrated.

About 40 nanolatex films were prepared for some kinetic experiments by coating a similarly polymerized 4% ILBr dialyzed nanolatex dispersion at a  $150\ \mu\text{m}$  wet film thickness on microscope slides. On drying overnight coalesced films formed of about  $10\ \mu\text{m}$  thickness. On exposing one of these samples to 0.1 M aqueous  $\text{KPF}_6$  solution for another 24 h, the film turned opaque and porous, was washed with DI water, dried, and then peeled off of the slide substrate. The SEM in Figure 4 shows many through-film pores about  $5\ \mu\text{m}$  diameter

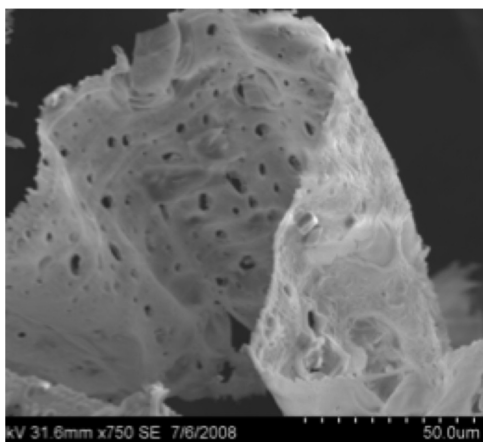


Figure 4. Porous film peeled from microscope slide substrate.

and more, suggesting that ultimately the poration becomes sufficiently substantial to weaken adhesion to the substrate.

Other of these slides were then exposed to aqueous 0.1 M  $\text{KPF}_6$  for an interval varying from 1 min to 40 h. After exposure the films were washed in DI water and dried. Their turbidity was then measured at 800 nm by measuring the absorbance relative to an uncoated microscope slide control in the reference beam. This ILBr/MMA copolymer has no intrinsic absorbance at 800 nm, so the apparent optical density is a good measure of turbidity. The three series of sequential exposures illustrated in Figure 5 show that there appears to be an induction period of about 2–4 h where the turbidity increases slowly. After this time the turbidity appears to increase more rapidly over the 40 h test period. Because the turbidity appears not to have saturated, we surmise that maximum poration is achieved only at longer treatment times.

The change in lightness<sup>23</sup> (relative reflectance), dL, upon poration was examined by preparing a series of dialyzed nanolatex films on aluminum panels by an automatic draw down applicator to produce a wet film thickness of  $200\ \mu\text{m}$ . The films were then allowed to dry and coalesce overnight. They were then exposed to aqueous 0.1 M  $\text{KPF}_6$  for various time intervals, rinsed, and dried overnight again. The lightness value for the first film which was exposed to  $\text{KPF}_6$  for 1 min was used as a reference and changes in lightness for all the

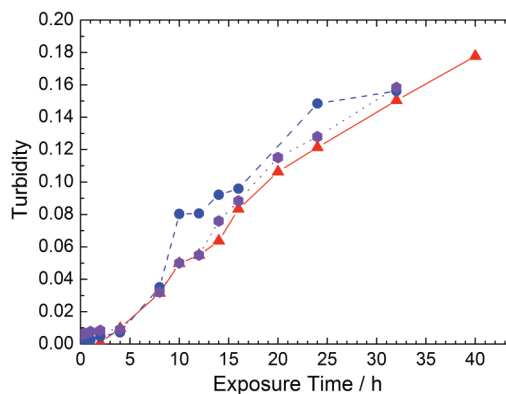


Figure 5. Turbidity as a function of exposure time to aqueous 0.1 M  $\text{KPF}_6$  solution for ILBr latex films on glass. Each of the three symbol types represents a distinct experimental series.

other films were determined against the first film. The lightness values were obtained using a hand-held BYK Gardner Colorguide ( $45^\circ/0^\circ$ ). The results are presented in Figure 6 where it

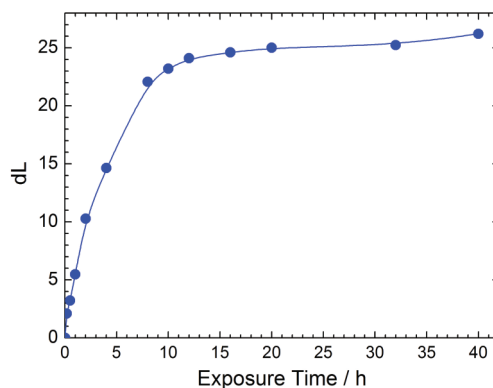


Figure 6. Lightness (dL) as a function of exposure time to aqueous 0.1 M  $\text{KPF}_6$  solution for ILBr nanolatex films on aluminum substrate.

is seen that qualitatively different behavior is obtained by this reflectance technique in comparison to the transmission (turbidity) data of Figure 5.

From Figures 5 and 6 we can conclude that the initial poration is localized on the surface and that the proportion of light scattered and transmitted forward (Figure 5) into the detector decreases only slightly over the 0–4 h exposure interval, while the dL values indicate the light scattered backward increases steadily over this same time interval and longer. Both figures also suggest a break point in the respective data in the 2–2.5 h interval. This combination of turbidity and reflectance data is consistent with the main changes being confined to the top surface of the coatings at early exposure times. As poration increases with further exposure, the transmittance steadily decreases, and the reflectance steadily increases as the bulk film becomes more porous. The reflectance appears to reach an asymptotic limiting value at about 20–30 h exposure. The bulk poration appears still to be increasing at 40 h exposure. SEM of various surfaces of these samples peeled from the slides are given in the SI.

These films demonstrate that transparent coatings can be produced from poly(ILBr/MMA) nanolatexes and transformed into an opaque, porous state by treatment with aqueous  $\text{KPF}_6$ . These films also demonstrate the feasibility of creating porous

membranes by painting stimuli-responsive nanolatexes on a suitable substrate and then treating the film with a stimulus-responsive anion (e.g.,  $\text{BF}_4^-$ ,  $\text{PF}_6^-$ , or  $\text{N}(\text{CN})_2^-$ ).

This poration behavior is nearly identical to that observed for aqueous gels produced from the same monomers and treated with the same anions. We previously found those lightly cross-linked gels to be pinned for reversible spinodal decomposition. In this coalesced nanolatex system, however, it is hard to imagine intrinsic network structures larger than the 20–30 nm nanolatexes. One possibility, speculatively speaking, may be the interdigitated internanolatex chains forming a network of interconnected “facets” “between” coalesced nanolatex particles (see TEM in SI). While such a “network” reasonably extends over the dimensions of the film, we cannot yet imagine how it might set boundaries on pore dimensions.

Quite recently, Yuan and Antonietti<sup>24</sup> described a new family of similarly sized nanolatexes (20–37 nm) polymerized from aqueous micellar solutions of 1-vinyl-3-alkyl imidazolium bromide surfactants (and ionic liquid monomers) with octyl through octadecyl alkyl substituents and using a 1,4-butanediyl-3,3'-bis-1-vinylimidazolium dibromide cross-linking agent. Stable nanolatexes were obtained for the  $\text{C}_{12}$ ,  $\text{C}_{14}$ ,  $\text{C}_{16}$ , and  $\text{C}_{18}$  substituted monomers without the cross-linker and for the  $\text{C}_{14}$ ,  $\text{C}_{16}$ , and  $\text{C}_{18}$  substituted monomers with 10 mol % cross-linker. As an example, the nanolatex deriving from the  $\text{C}_{14}$  monomer with cross-linker was examined in aqueous KBr and found to be unstable above 0.03 M aqueous. They contrasted this behavior with the stability illustrated initially<sup>11</sup> and noted the structural differences and that the monomer ratios and types may be responsible for the different salt sensitivities. Here we show our nanolatexes stable at 6-fold this coagulation concentration of 0.03 M, but these differences may very well also be due to the high charge density on their latex backbone homopolymers, as Yuan and Antonietti pointed out,<sup>24</sup> wherein the cationic imidazolium groups are all adjacent to the backbone. It will be interesting to discover if such nanolatexes also are responsive to anions such as  $\text{BF}_4^-$ ,  $\text{PF}_6^-$ , and  $\text{CF}_3\text{SO}_3^-$ , as are a variety of imidazolium-based polymerized ionic liquids.<sup>22</sup>

In our nanolatexes, with a molar ratio of ILBr/MMA of about 1:2.6 used in the formulation, the charge density is depressed as was pointed out,<sup>24</sup> because MMA monomers may be randomly interspersed among the ILBr monomers. Further, the imidazolium bromide group is distal to the backbone. We suspect our nanolatex copolymer chains are akin to osmotic spheres,<sup>25,26</sup> wherein the bromide counterions are osmotically trapped within the nanolatex hydrogel particles. The aquated and water swollen copolymer strands undergo very soft and ionic liquid kinds of weak repulsive interactions upon collision rather than a hard electrostatic interaction more typical of nonhydrogel colloids. In support of this conjecture, we note that the second ionic liquid polymer of an ionic liquid monomer to be reported,<sup>27,28</sup> the polyILBF<sub>4</sub> homopolymer, is not very water-soluble but forms an ionic liquid melt phase above 30 °C.

Classical ionic-strength-induced coagulation does not rely upon specific counterion interactions with the latex. We have shown here that these nanolatexes are destabilized by 0.35 mM  $\text{PF}_6^-$ . This concentration is 300-fold more dilute than 0.1 M  $\text{Br}^-$ . Additionally, our nanolatexes are stable in 1 M  $\text{Na}_2\text{S}$ , which exhibits an ionic strength of 3 M, 8600-fold higher than 0.35 mM  $\text{PF}_6^-$ .

These poly(ILBr/MMA) nanolatexes represent a new class of very stable and soft ionic nanogels. These ionic nanogels appear to be osmotic nanospheres that exhibit ionic strength insensitivity.<sup>25,29,30</sup> Pincus pointed out<sup>25</sup> that many colloid applications could use stabilization that is not sensitive to Debye–Hückel screening effects. These nanogels exhibit this positive characteristic and, in addition, have been shown to be excellent stabilizers for waterborne nanocarbons.<sup>31–34</sup>

These anion-specific effects on imidazolium groups have been observed in a number of studies focusing on various kinds of supramolecular complexes,<sup>35–37</sup> exchange resins,<sup>38</sup> and polymers aimed at developing anion sensors<sup>39</sup> and quantitative analyses.<sup>40</sup> A logical conclusion following from the anion-sensitive stimuli responsiveness of imidazolium-containing polymerized ionic liquids and the above-mentioned anion sensing studies is that this stimuli responsiveness emanates from anion-imidazolium ion pairing. Further, in a recent study<sup>41</sup> it was shown that the homopolymer of polyILBr prepared by a heterogeneous ATRP process condenses upon addition of  $\text{KPF}_6$  to form nanoparticles of polyILPF<sub>6</sub>. The  $K_{\text{sp}}$  of the ILPF<sub>6</sub> monomer was estimated as  $6 (\pm 2) \times 10^{-7}$  M, as precipitated in water at room temperature.<sup>18</sup>

To explain the insensitivity to conventional Debye–Hückel screening effects leading to indifferent electrolyte coagulation, we at present rely upon the osmotic nanosphere structure inferred above from the polymer brush literature. The osmotically trapped counterions within the osmotic nanospheres have a local concentration of the order of 0.1 M or greater (see SI). The exterior indifferent electrolyte will tend to cause the osmotic spheres to swell (limited by extant cross-linking) at low electrolyte and to condense at high electrolyte. Such spheres interact softly and repulsively. Excess indifferent electrolyte cannot markedly affect the osmotic sphere unless interactions with the imidazolium ring are strong enough to displace the  $\text{Br}^-$ . When such an interaction is strong, as in the present case, the change from hygroscopic to hydrophobic produces spinodal decomposition and the accompanying pore formation.

We hasten to point out this study is not the first reported case of colloidal stability being dictated by specific chemical effects rather than by indifferent electrolyte. Phosphate and sulfate have been shown to strongly adsorb to surface sites in hematite<sup>42</sup> and aluminum oxide<sup>43</sup> dispersions, respectively. These interactions strongly modify (decrease) the intrinsic surface potential and lead to coagulation of particles.

Latex films devoid of porogens appear not to have been associated with membrane formation previously. Here we have bottom-up self-assembly<sup>44</sup> to construct a film via an as yet uncharacterized coalescence mechanism. Such stimuli-responsiveness, enabling switching from a gel state to a locally phase-separated state, establishes nanolatex film formation and ion exchanging with an appropriate anion as a two-step process to coat macroscopic materials with nano, meso, and microscopically porous membranes.

We anticipate such nanogels will prove useful in fabricating diverse membranes<sup>45,46</sup> having porosity on different length scales. Besides the intrinsic poration available from the films demonstrated here, the use of such nanogels to infuse photonic and related larger particle templates may result in new manufacturing processes for diffusion and other membranes for batteries and fuel cells.

## ■ ASSOCIATED CONTENT

### ● Supporting Information

Synthesis, turbidity-salt effects, film formation, TEM, thermal analysis, mechanical analysis, and SEM of porous films are described. This material is available free of charge via the Internet at <http://pubs.acs.org>.

## ■ AUTHOR INFORMATION

### Corresponding Author

\*E-mail: [jtexter@emich.edu](mailto:jtexter@emich.edu).

### Present Addresses

<sup>†</sup>Specialty Coating Systems, 7645 Woodland Drive, Indianapolis, Indiana, 46278, United States.

<sup>‡</sup>Asian Paints Ltd., Research and Technology Center, Plot No C3-B/1, TTC MIDC Pawane, Thane Belapur Road, Navi Mumbai (New Bombay) 400705, India.

### Notes

The authors declare the following competing financial interest(s): John Texter has an equity interest in a pending U.S. Patent Application, US 2011/0233458 A1, 29 September 2011; "Nanoparticle dispersions with ionic liquid-based stabilizers."

## ■ ACKNOWLEDGMENTS

This work was supported by AFOSR Grant Award No. FA9550-08-1-0431 and WPAFB UTC Prime Contract FA8650-05-D-5807, Task Order BH Subcontract Agreement 06-S568-BH-C1), by Army Research Laboratory Contract No. W911QX-06-C-0102, and by ONR Grant Award No. N00014-04-1-0763. This work was further supported by instrumentation grants from the United States National Science Foundation (Grant Nos. DMR-0414803 and CHE-0443444). We thank Dr. Zhiming Qiu for providing the transmission electron micrographs (SI).

## ■ REFERENCES

- (1) Kassner, H.; Siegert, R.; Hathiramani, D.; Vassen, R.; Stoeber, D. *J. Thermal Spray Technol.* **2008**, *17*, 115–123.
- (2) Edwards, M. O. M.; Andersson, M.; Gruszecki, T.; Pettersson, H.; Thunman, R.; Thuraisingham, G.; Vestling, L.; Hagfeldt, A. *J. Electroanal. Chem.* **2004**, *565*, 175–184.
- (3) Biswas, P. K.; Sujatha Devi, P.; Chakraborty, P. K.; Chatterjee, A.; Ganguli, D. *J. Mater. Sci. Lett.* **2003**, *22*, 181–183.
- (4) Kum, B. G.; Park, Y. C.; Chang, Y. J.; Jeon, J. Y.; Jang, H. M. *Thin Solid Films* **2011**, *11*, 3778–3781.
- (5) Fogden, A. Coll.; Surf., A. *Physicochem. Eng. Aspects* **2009**, *349*, 102–109.
- (6) Gao, J.; Li, X.; Han, Y. *Polymer* **2010**, *51*, 2683–2689.
- (7) Park, M. S.; Lee, Y.; Kim, J. K. *Chem. Mater.* **2005**, *17*, 3944–3950.
- (8) Stanislawski, A.; LePoutre, P. In *Technology for Waterborne Coatings*; Glass, J. E., Ed.; ACS Symposium Series; American Chemical Society: Washington, DC, 1997; Vol. 663, pp 226–244.
- (9) Ridgeway, C. J.; Schoelkopf, J.; Gane, P. A. C. *Transp. Porous Media* **2011**, *86*, 945–964.
- (10) Jiang, H.; Zhao, W. Z.; Li, C. L.; Wang, Y. C. *Polymer* **2011**, *52*, 778–785.
- (11) Yan, F.; Texter, J. *Chem. Commun.* **2006**, 2696–2698.
- (12) Abbas, Z.; Gunnarsson, M.; Ahlberg, Nordholm, S. *J. Colloid Interface Sci.* **2001**, *243*, 11–30.
- (13) Einarson, M. B.; Berg, J. C. *J. Colloid Interface Sci.* **1993**, *155*, 165–172.

- (14) Hidalgo-Alvarez, R.; Martin, A.; Fernandez, A.; Bastos, D.; Martinez, F.; delas Nieves, F. J. *Adv. Colloid Interface Sci.* **196**, *67*, 1–118.
- (15) Yan, F.; Texter, J. *Angew. Chem., Int. Ed.* **2007**, *46*, 2440–2443.
- (16) Co, C. C.; de Vries, R.; Kaler, E. W. In *Reactions and Syntheses in Surfactant Systems*; Texter, J., Ed.; Marcel Dekker: New York, 2001; pp 455–469.
- (17) Yan, F.; Texter, J. *Soft Matter* **2006**, *2*, 109–118.
- (18) England, D. MS Thesis, Eastern Michigan University, 2008.
- (19) Vijayakrishna, K.; Jewrajka, S. K.; Ruiz, A.; Marcilla, R.; Pomposo, J. A.; Mecerreyes, D.; Taton, D.; Gnanou, Y. *Macromolecules* **2008**, *41*, 6299–6308.
- (20) Vijayakrishna, K.; Mecerreyes, D.; Gnanou, Y.; Taton, D. *Macromolecules* **2009**, *42*, 5167–5174.
- (21) Yan, F.; England, D.; Gu, H.; Texter, J. In *Smart Coatings III*; Baghdachi, J.; Provder, T., Eds.; American Chemical Society: Washington, DC, 2010; Ch. 13, pp 191–207; ACS Symposium Series; American Chemical Society: Washington, DC, 2010; Vol. 1050, pp 191–207.
- (22) Mecerreyes, D. *Prog. Polym. Sci.* **2011**, *36*, 1629–1648.
- (23) Mitterer, C.; Komenda-Stallmaier, J.; Losbichler, P.; Schmoetz, P.; Stori, H. *Surf. Coat. Technol.* **1995**, *74–75*, 1020–1027.
- (24) Yuan, J.; Antonietti, M. *Macromolecules* **2011**, *44*, 744–750.
- (25) Pincus, P. *Macromolecules* **1991**, *24*, 2912–2919.
- (26) Jusufi, A.; Likos, C. N.; Löwen, H. *J. Chem. Phys.* **2002**, *116*, 11011–11027.
- (27) Gu, H. MS Thesis, Eastern Michigan University, 2009.
- (28) Yan, F.; Lu, J.; Texter, J. *Prog. Polym. Sci.* **2009**, *34*, 431–444.
- (29) Gottwald, D.; Likos, C. N.; Kahl, G.; Löwen, H. *J. Chem. Phys.* **2005**, *116*, 074903.
- (30) Denton, A. R. *Phys. Rev. E* **2003**, *67*, 011804.
- (31) Antonietti, M.; Shen, Y.; Nakanishi, T.; Manuelian, M.; Campbell, Gwee, L.; Elabd, Y.; Tambe, N.; Crombez, R.; Texter, J. *ACS Appl. Mater. Interfaces* **2010**, *2*, 649–653.
- (32) Zhao, L.; Crombez, R.; Antonietti, M.; Texter, J.; Titirici, M.-M. *Polymer* **2010**, *51*, 4540–4546.
- (33) Giordano, C.; Yang, W.; Lindemann, A.; Crombez, R.; Texter, J. *Colloids Surf., A* **2011**, *374*, 84–87.
- (34) Texter, J.; Crombez, R.; Ma, X.; Zhao, L.; Perez-Caballero, F.; Titirici, M.-M.; Antonietti, M. *Prepr. Symp.-Am. Chem. Soc., Div. Fuel Chem.* **2011**, *56*, 388–389.
- (35) Alcade, E.; Dinares, I.; Mesquida, N. *Top. Heterocycl. Chem.* **2010**, *24*, 267–300.
- (36) Xu, Z.; Choi, J. Y.; Yoon, J. *Bull. Korean Chem. Soc.* **2011**, *32*, 1371–1374.
- (37) Vickers, M. S.; Martindale, K. S.; Beer, P. D. *J. Mater. Chem. Soc.* **2005**, *15*, 2784–2790.
- (38) Alcade, E.; Dinares, I.; Ibañez, A.; Mesquida, N. *Eur. J. Org. Chem.* **2011**, 298–304.
- (39) Chen, X.; Kang, S.; Kim, M. J.; Kim, J.; Kim, Y. S.; Kim, H.; Chi, B.; Kim, S.-J.; Lee, J. Y.; Yoon, J. *Angew. Chem., Int. Ed.* **2010**, *49*, 1422–1425.
- (40) Zhao, J.; Yan, F.; Chen, Z.-Z.; Diao, H. B.; Chu, F. Q.; Yu, A. M.; Lu, J. M. *J. Polym. Sci., Part A: Polym. Chem.* **2009**, *47*, 746–753.
- (41) Ma, X.; Ashaduzzaman, Md.; Kunitake, M.; Crombez, R.; Texter, J.; Slater, L.; Mourey, T. *Langmuir* **2011**, *27*, 7148–7157.
- (42) Chorover, J.; Zhang, J.; Amistadt, M. K.; Buffle, J. *Clays Clay Miner.* **1997**, *45*, 690–708.
- (43) Waite, T. D.; Cleaver, J. K.; Beattie, J. K. *J. Colloid Interface Sci.* **2001**, *241*, 333–339.
- (44) Texter, J.; Tirrell, M. *AIChE J.* **2001**, *47*, 1706–1710.
- (45) Texter, J. C. R. *Chim.* **2003**, *6*, 1425–1433.
- (46) Texter, J. *Prog. Coll. Polymer Sci.* **2009**, *287*, 313–321.